Fluctuating fluid flow and heat transfer measurements of an impinging air jet

Tadhg S. O'Donovan, Darina B. Murray

Mechanical & Manufacturing Engineering, Trinity College Dublin, Ireland, tadhg.odonovan@tcd.ie

Abstract Impinging air jets are known to yield relatively high local and area averaged convective heat transfer coefficients and can be used for the cooling of electronic components, gas turbine blades and manufacturing processes such as grinding. The current research is concerned with the measurement of fluid flow and heat transfer to an impinging air jet. This investigation was limited to a Reynolds Number, (Re) of 10000 and nozzle to impingement surface distance, (H/D) from 1.0 to 2.0. Both mean and fluctuating heat transfer profiles are presented for the range of variables considered. Heat transfer distributions exhibit secondary peaks at a radial position which is dependent on H/D. The secondary peaks in the mean Nusselt number distribution are a result of an abrupt increase in turbulence in the wall jet boundary layer. Laser Doppler Anemometry has been used to acquire time resolved velocity measurements. Spectral and coherence information of the individual velocity and heat transfer signals is presented. It has been shown that fluctuations in the fluid velocity close to the impingement surface correlate well with the heat transfer from the surface. It has been shown also that vortices which are responsible for introducing regular velocity fluctuations in the transitional wall jet region can influence the magnitude of the heat transfer coefficient. The evolution of vortices in the impingement jet flow has been discussed. It has been shown that the break-up of vortices in the wall jet increases the magnitude of the velocity fluctuations normal to the impingement surface. It has also been shown that vortices at an early stage of their development enhance the heat transfer in the wall jet contributing to the magnitude of the secondary peak in the heat transfer distribution.

1. Introduction

Impinging jets have been used to transfer heat in diverse applications, which include the cooling of electronic components, gas turbine blades and manufacturing processes such as grinding. Hollworth and Durbin [1] investigated the impingement cooling of electronics. Roy et al. [2] investigated the jet impingement heat transfer on the inside of a vehicle windscreen and Babic et al. [3] used jet impingement for the cooling of a grinding process. The main variables for jet impingement heat transfer are the angle of impingement, the jet Reynolds number and the height of the nozzle above the impingement surface. A comprehensive review of heat transfer to an impinging circular jet has been conducted by Jambunathan et al. [4]. Martin [5] also conducted a review of jet impingement heat transfer for a wider range of parameters that included jet arrays, confinement and submergence. Polat et al. [6] also presented a review of numerical investigations that have been conducted in the area of convective heat transfer to impinging jets. Comprehensive studies of the mean fluid flow characteristics of both free and impinging jets have also been presented by Donaldson and Snedeker [7], Beltaos [8] and Martin [5].

In many investigations, including one by Gardon and Akfirat [9], the heat transfer to an impinging jet has been correlated with what is often termed the "arrival flow condition". This is the flow condition at an equivalent location in a free jet. It is well established that the shape of the heat transfer distribution changes significantly with nozzle to impingement surface spacing. In studies by Baughn and Shimizu [10], Huang and El-Genk [11], Goldstein et al. [12], O'Donovan et al. [13] and others, secondary peaks in the heat transfer distribution have been reported for a jet impinging at low nozzle to surface spacing ($H/D \leq 2$). According to Hoogendoorn [14] for a jet with low turbulence, two radial peaks occur in the heat transfer distributions. Goldstein and Timmers [15] compared heat transfer distributions of a large nozzle to plate spacing ($H/D = 6$) to that of a relatively small spacing ($H/D = 2$). It was shown that while the Nusselt number decays from a peak

at the stagnation point for the large *H/D*, the Nusselt number is a local minimum at the stagnation point when $H/D = 2$. For the same jet Reynolds number the average heat transfer coefficient was found to be lower for the smaller nozzle to surface spacing; this was attributed to the fact that the mixing induced in the shear layer of the jet had not penetrated to the potential core of the jet. The flow within the potential core has relatively low turbulence and consequently the heat transfer is lower in this case. Goldstein et al. [12] continued research in this area. Once again, at small spacings ($H/D \leq 5$), secondary maxima were evident at a radial location in the heat transfer distribution; at $H/D = 2$ these maxima were greater than the stagnation point Nusselt number. The secondary maxima occur at approximately *r/D* of 2 and were attributed to entrainment caused by vortex rings in the shear layer. Several investigators including Donaldson et al. [16] presented heat transfer data for a jet impinging at very large *H/D*. According to Mohanty and Tawfek [17] the heat transfer rate peaks at the stagnation point and decreases exponentially with increasing radial distance beyond $r/D = 0.5$ for $4 < H/D < 58$.

In more recent years research in this area has been concerned with the vortical nature of the impinging jet flow. In a jet flow vortices initiate in the shear layer due to Kelvin Helmholtz instabilities. Vortices, depending on their size and strength, affect the jet spread, the potential core length and the entrainment of ambient fluid. Fleischer et al. [18] employed a smoke wire technique to visualise the initiation and development of a vortex in an impinging jet flow. The vortex break-up location indicated a transition to turbulent flow that cannot sustain large scale flow structures. At large *H/D* the vortices break-up as they reach the end of the potential core, before impinging on the surface. This occurs following a vortex merging process where the size of the vortex increases but the strength decreases. Vortices merge because the vortex does not move fast enough to prevent being entrained by the fluid flow. Hui et al. [19] and Hussain [20] describe the break-up process of a vortex.

Artificial jet excitation can control the development of vortices in the jet flow and therefore is thought to have the potential to enhance the heat transfer from the surface. Liu and Sullivan [21] excited an impinging air jet acoustically and reported on the resulting flow and heat transfer distributions. It has been shown that, depending on the frequency of excitation, the area averaged heat transfer can be enhanced or reduced at low nozzle to impingement surface spacings. In the case where the jet is excited at a subharmonic of the natural frequency of the jet, the heat transfer is reduced. This frequency has the effect of strengthening the coherence of the naturally occurring frequency. The jet was also excited at a frequency higher than that of the natural jet frequency. In this case the excitation had the effect of producing intermittent vortex pairing. This results in a break down of the naturally occurring vortex. Consequently, the transition to small scale turbulence effectively increases the heat transfer to the impinging air jet.

In recent times control of the jet flow vortices has attracted much research interest as the latest parameter identified to have a role to play in the heat transfer mechanisms. Hui et al. [19] and Gao et al. [22] installed mechanical tabs at the nozzle exit; these lead to streamwise vortical structures which increase the secondary instabilities in the jet and therefore hasten the “cut and connect” process that breaks the vortices down into small scale turbulence. Hwang et al. [23] investigated the effect of acoustic excitation on a coaxial jet flow and explored the resulting effect on the heat transfer. Hwang and Cho [24] continued this research for a wider range of test parameters. While the research to date has shown possible enhancement of the mean heat transfer at various excitation frequencies, much of this has been attributed to changes in the arrival velocities. The effect of the vortical flow structure on the local heat transfer has not been reported in depth.
The current research investigates the fluid flow and heat transfer for a submerged, unconfined axially symmetric impinging air jet. Of particular interest to the current investigation are the

secondary peaks that occur in the mean heat transfer distribution when the jet nozzle is placed within 2 diameters of the impingement surface. An important objective of the current research is to reveal the convective heat transfer mechanisms that influence the magnitude and location of these peaks. Control of the vortex development in the shear layer of the free jet and its influence on heat transfer has been a major area of interest in this field in recent years. It has been shown that by exciting the jet, acoustically or otherwise, the vortex development can be controlled and this has a consequence for heat transfer. This research illustrates the influence that various stages within the vortex development have on the convective heat transfer in the wall jet.

2. Experimental Rig

The main elements of the experimental rig are a nozzle and an impingement surface as shown in figure 1. The heated flat surface consists of a plate with three main layers, measuring 425mm x 550 mm. The top surface is a 5 mm thick copper plate. A silicon rubber heater mat, approximately 1.1 mm thick, is fixed to the underside of the copper plate with a thin layer of adhesive. It has a power rating of 15 kW/m^2 and a voltage rating of 230 V. The voltage is varied using a variable transformer that controls the heat supplied to the copper plate. A thick layer of insulation prevents heat loss from the heating element other than through the copper. The plate assembly approximates a uniform wall temperature boundary condition, operating typically at a surface temperature of 60°C. The nozzle consists of a brass pipe of 13.5 mm internal diameter. The pipe is 20 diameters long and a 45° chamfer is machined at the nozzle lip to create a sharp edge to minimize entrainment. The nozzle is clamped on a carriage in an arrangement that allows its height above the impingement surface to be varied, with a range from 0.5 to 8 nozzle diameters above the impingement surface.

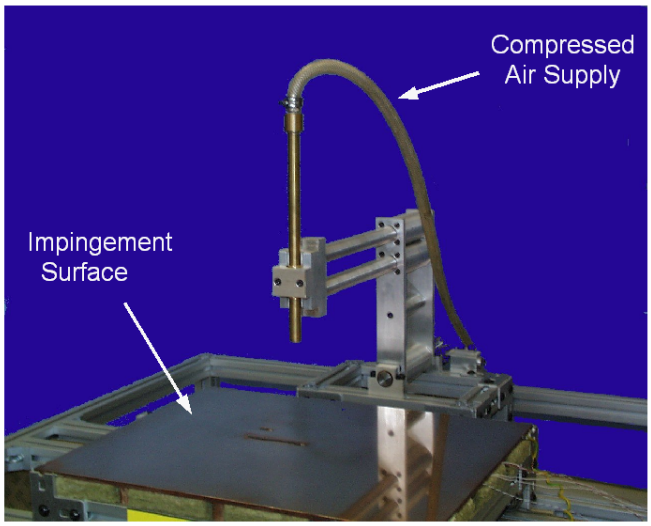

Figure 1: Experimental Rig

Air is supplied to the jet nozzle by a compressor. An Alicat Scientific Inc. Precision Gas Flow Meter is installed on the compressed air line to monitor both the air volume flow rate and temperature. Real time acquisition of the air volume flow rate allows for accurate setting of the jet exit Reynolds number, by varying a needle control valve also installed on the line, just prior to the flow meter. For this investigation the jet exit temperature is maintained within 0.5°C of the ambient air temperature by using a heat exchanger installed on the air line. The heat exchanger consists of a controlled temperature water bath in which a series of copper coils are placed. The air flows through the copper coils to increase the jet exit temperature to the required setting.

The impingement surface is instrumented with two single point heat flux sensors. These are an RdF Micro-Foil® heat flux sensor and a Senflex® Hot Film Sensor. T-type thermocouples are also placed

on the instrumented plate in the vicinity of the two heat flux sensors to measure the surface temperature locally. Finally, a thermocouple is placed in the jet flow line at the flow meter and another in the ambient air near the nozzle exit to monitor the entrained air temperature. The RdF Micro-Foil® heat flux sensor consists of a differential thermopile that measures the temperature above and below a known thermal barrier. The heat flux through the sensor is therefore defined by:

$$\ddot{q} = k_s \frac{\Delta T}{\delta}$$

where k_s is the thermal conductivity of the barrier (kapton) and ΔT is the temperature difference across the thickness (δ) of the barrier. A single pole thermocouple is also embedded in this sensor to measure the surface temperature locally. For the specific sensor thickness used the characteristic 62 % response to a step function is 0.02 s.

The Senflex® Hot Film Sensor operates in conjunction with a Constant Temperature Anemometer to measure the fluctuating heat flux to the impinging jet as it has higher temporal resolution than the Micro-Foil® sensor and can accurately acquire data up to 8 kHz. The sensor consists of a nickel sensor element that is electron beam deposited onto a 0.051 mm thick Upilex S polyimide film. The hot film element has a thickness of < 0.2 μm and covers an area of approximately 0.1 mm x 1.4 mm. The typical cold resistance of the sensor is between 6 and 8 Ohms. A TSI Model 1053B Constant Temperature Anemometer is used to control the temperature of the hot film. It maintains the temperature of the film at an overheat (≈ 5°C) above the heated surface. The power required to maintain this temperature is equal to the heat dissipated from the film. Thus, the voltage required to maintain the temperature of the film constant is proportional to the heat transfer to the air jet as described by:

$$q_{dissipated} \propto \frac{E_{out}^2}{R}$$

The constant of proportionality accounts for losses, including conduction to the impingement surface. Heat transfer results are presented in the form of mean and fluctuating Nusselt number distributions that have calculated uncertainties of 5.7 % and 30.0 % respectively. These are based on the local heat transfer coefficient that is defined by:

$$h(r) = \frac{\ddot{q}(r)}{T_{surf}(r) - T_j}$$

Where $\ddot{q}$ is the heat flux from the surface, T_j is the jet exit temperature and T_{surf} is the local surface temperature. These uncertainties are based on a worst case scenario where the uncertainty is a percentage of the smallest measurements; it is clear from the results presented here that the uncertainty in Nu' are, in general, less than 30 %. A complete calibration and uncertainty analysis for this experimental set-up is presented by O'Donovan [25].

Laser Doppler Anemometry is employed as a non-intrusive method of measuring the flow velocity close to the impingement surface. Food grade polyfunctional alcohol liquid seeding particles, typically 1 to 50 μm in diameter, were used to seed both the jet flow and the ambient air. The Laser Doppler Anemometry system is based on a Reliant 500 mW Continuous Wave laser from Laser Physics. This is a two component system and therefore the laser is split into 2 pairs of beams, that have wavelengths of 514.5 nm (green) and 488 nm (blue), to measure the velocity in orthogonal directions at the same point location. The four beams, each of diameter 1.35 mm, are focused on a

point 250 mm from the laser head. The system works in backscatter mode and a Base Spectrum Analyser (BSA) acquires and processes the signal to compute the velocity. The signal has been re-sampled using Sample and Hold and a correction for error is preformed according to Fitzpatrick and Simon [26].

3. Results & Discussion

Both mean and fluctuating Nusselt number distributions for an impinging air jet are presented in figure 2. For this low range of H/D the Nusselt number is a maximum at the stagnation point (r/D = 0). With increasing radial distance the Nusselt number decreases from this maximum but rises again to a secondary peak. This has been attributed to the transition of the wall jet boundary layer to a fully developed turbulent flow. Beyond this peak the heat transfer distribution decays with increasing radial distance from the stagnation point. This is due to the increasing temperature and decreasing velocity of the wall jet flow.

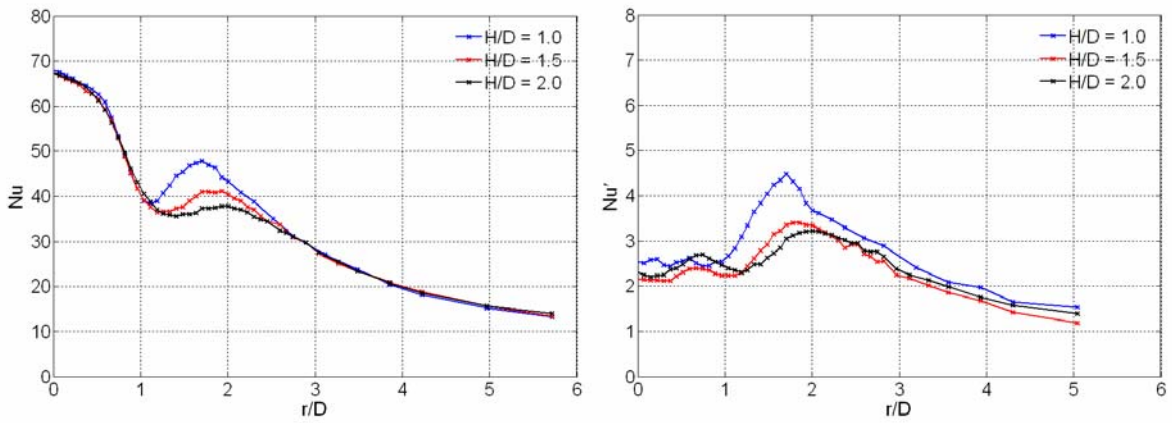

Figure 2: Mean & Fluctuating Nusselt Number Distributions; Re = 10,000

It has been shown by Liu and Sullivan [21] that the passing frequency of vortices in an impinging jet flow has an influence on the area averaged heat transfer distribution and in particular the magnitude of the secondary peak. To investigate such an effect, the fluctuating characteristic of the velocity at the jet exit was examined. Selected velocity spectra in both the radial and axial direction at the jet exit are presented in figure 5.26. The frequency (f) of velocity fluctuations is presented in the non-dimensional form of the Strouhal number, defined by:

$$St = \frac{fD}{U_{jet}}$$

where U_{jet} is the jet exit velocity. The velocity spectra at the centreline of the jet and in the shear layer are shown in figure 3. At both the centreline and shear layer locations the spectral power density is lower for the radial velocity component. This indicates that the velocity fluctuations are greatest in the main jet flow (axial) direction. Overall, however, the spectral power is far greater in the shear flow as this is a location of high turbulence. It is apparent that no dominant frequency appears in the jet centreline flow and that the velocity fluctuations reflect random small scale turbulence. In the shear layer, however, three dominant peaks in the power spectrum are evident at Strouhal numbers of approximately 0.6, 1.1 and 1.6 respectively. Schadow and Gutmark [27] reported similar frequencies that occur at the exit of their jet. The highest of the three frequencies was attributed to the frequency at which vortices roll up in the shear layer.

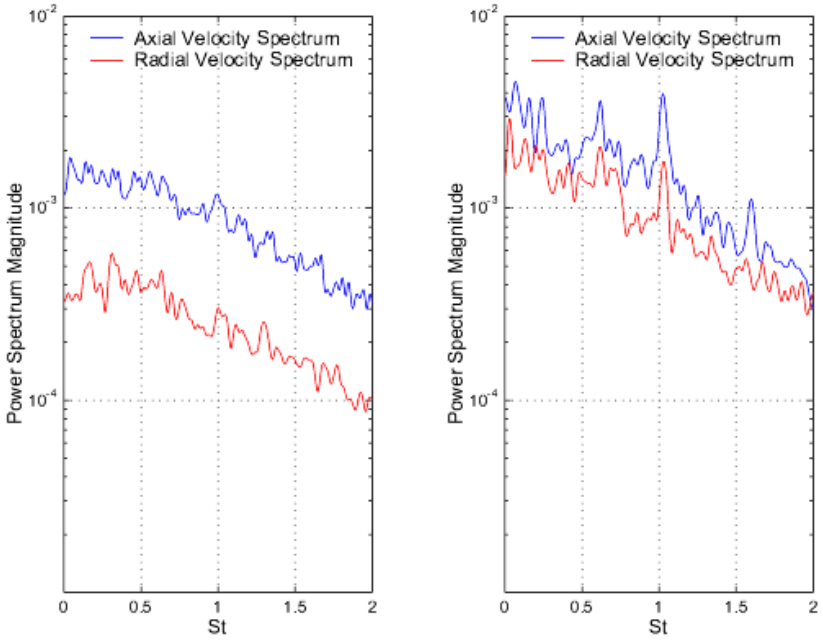

(a) Centreline, r/D = 0 **(b) Shear Layer, r/D = 0.4**

Figure 3: Free Jet Velocity Spectra, x/D = 0.5

Both of the lower frequencies are attributed to the frequencies at which vortices pass following merging processes. In an investigation by Han and Goldstein [28], two peaks were found in the velocity spectra. The higher frequency peak was attributed to the roll-up or passing frequency of the vortex. The lower frequency peak, however, only occurred at larger distances from the nozzle exit and was attributed to vortex pairing. In the current investigation it is thought that vortex merging occurs earlier due to the relatively high turbulence at the jet exit.

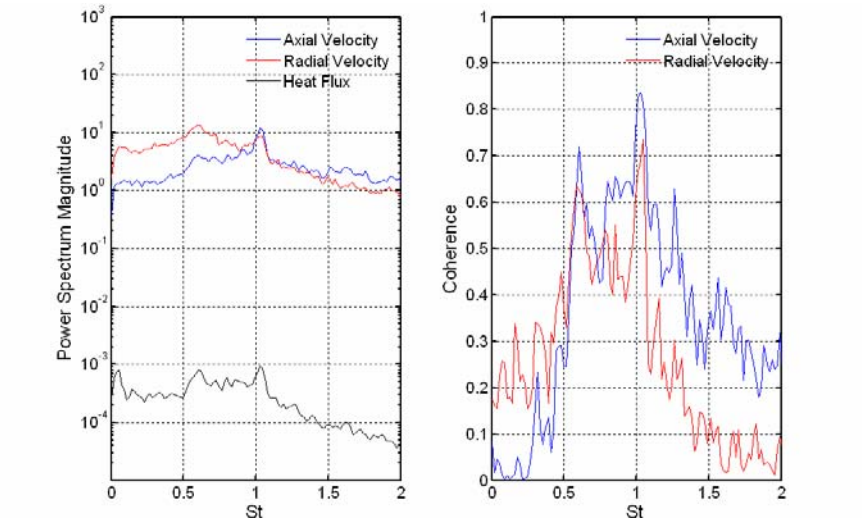

Figure 4: Spectral and Coherence Information; *Re* = 10000, *H/D* = 1.0, *r/D* = 1.0

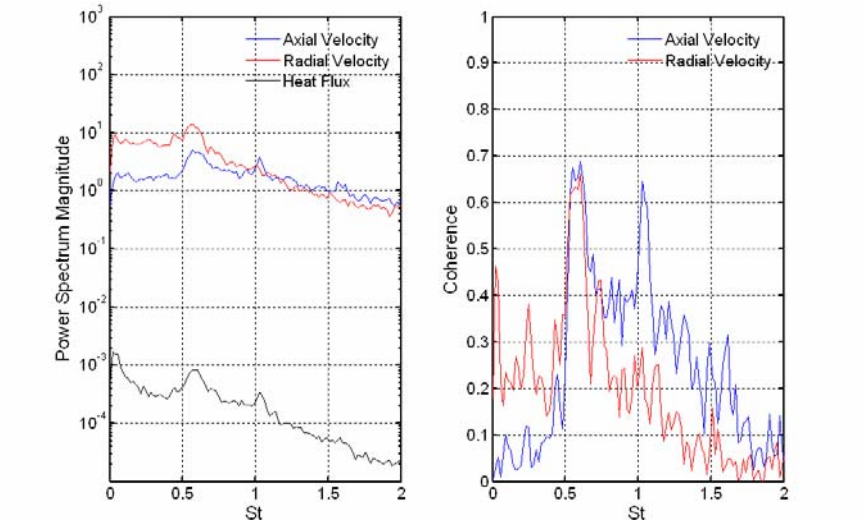

Figure 5: Spectral and Coherence Information; *Re* = 10000, *H/D* = 1.5, *r/D* = 1.0

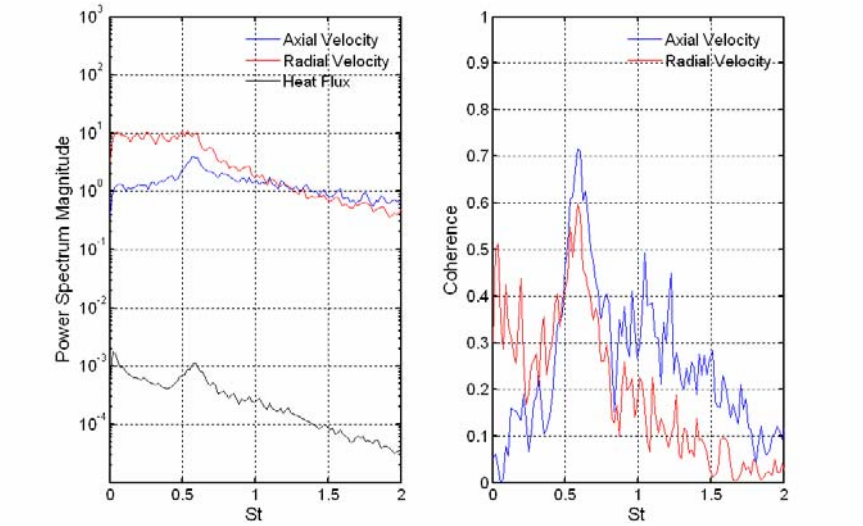

Figure 6: Spectral and Coherence Information; *Re* = 10000, *H/D* = 2.0, *r/D* = 1.0

Simultaneous measurements of the surface heat transfer and fluid flow 3mm above the surface reveal the extent to which the heat transfer depends on the local fluid flow. A trigger mechanism ensured the simultaneous acquisition of both fluid velocity and heat transfer signals. Spectral and coherence information for the velocity and heat flux signals at a radial location of r/D = 1.0 for jet impingement at H/D = 1.0, 1.5 and 2.0 are presented in figures 4, 5 and 6 respectively. This radial position was chosen as it is the location where the vortex impinges on the surface.

At H/D = 1 the three frequency peaks occur at Strouhal numbers of 0.6, 1.1 and 1.6. The Strouhal number of 1.1 corresponds to the frequency of the vortex resulting from the merging process of higher frequency vortices (St = 1.6), which were evident at the exit of the free jet. The peak at a Strouhal number of 1.6 is small in all three signals, indicating that the vortices which rolled up at the jet nozzle have merged to form larger vortices at a lower frequency. This new vortex is also undergoing a second merging process and this results in a peak at the low Strouhal number of 0.6. The radial velocity spectrum indicates that the two frequency peaks have similar magnitudes suggesting that the second vortex merging process is in progress. The axial velocity spectrum

however, shows the peak at the higher frequency to have the greater magnitude, suggesting that this vortex merging is in its initial stages.

For H/D = 1.5 two dominant peaks are evident in the individual spectra at St = 0.6 and 1.1 (figure 5). In general the two peaks have similar magnitudes indicating that the second vortex merging process is in progress. Once again, the spectrum of the radial velocity indicates that the vortex merging process is further advanced as the peak at the lower Strouhal number of 0.6 has the greater magnitude. Also, the coherence between the radial velocity and the heat flux is low at the higher Strouhal number (St = 1.1), indicating that the influence on heat transfer of velocity fluctuations normal to the impingement surface is greater.

At H/D = 1.5 and 2 the Strouhal number of 1.6 is no longer evident in the spectra suggesting that the initial merging process is complete. At these larger nozzle to impingement surface spacings the vortices have grown in size due to the vortex merging process. Finally, at H/D = 2 only one dominant peak remains in all three spectra, at a Strouhal number of 0.6. At this stage it is apparent that the second merging process has completed to form one large vortex. The large scale vortices pass at this lower frequency and determine the frequency of the jet column instability to correspond to a Strouhal number of 0.6. According to Broze and Hussain [29], this Strouhal number is consistent with the natural frequency that is expected for a jet that issues with a turbulence level of approximately 30 %.

In general, it has been shown that for a normally impinging jet with $H/D \leq 2$ the heat flux exhibits a significant dependence on velocity fluctuations normal to the impingement surface. Even in cases where velocity fluctuations parallel to the surface are greater than normal to the surface, the heat transfer relies substantially on the axial fluctuations. The variation of H/D from 1 to 2 has seen vortices at different stages of their development impinge upon the heated surface. At H/D = 1 the vortices are strong and initiate and pass at high frequencies. At larger H/D the vortices merge, and pass along the wall jet at lower and lower frequencies.

It has been shown to date that fluctuations in the radial direction have less of an influence on the heat transfer than the fluctuations normal to the impingement surface. At the different nozzle heights above the impingement surface the velocity fluctuations normal to the impingement surface have changed significantly. It has been shown by O'Donovan et al. [13] that the mean velocity distributions in the wall jet of an impinging jet flow are similar for the range of H/D considered. In fact, the only appreciable difference in the wall jet flow is the magnitude of the velocity fluctuations normal to the impingement surface, which decrease with increasing H/D. Therefore the variation in the velocity fluctuations can be attributed to the variation in the vortical nature of the impinging jet flow. The subsequent break-up of vortices in the wall jet induces velocity fluctuations normal to the impingement surface that increase surface heat transfer. It is concluded therefore that, when a vortex impinges at the early stage of its development, it is strong and maintains the low turbulence in the wall jet. Break-up of this strong vortex, however, results in large axial velocity fluctuations that enhance the mean surface heat transfer. When the vortex impinges on the surface at later stages of its development, its effects are less pronounced. The break-up of this weaker vortex results in lower magnitude axial velocity fluctuations and therefore does not increase the surface heat transfer to the same extent.

Vortices that impinge upon the surface determine the magnitude and frequency of the fluctuations in both directions. Because of this, the various stages of the vortex merging process influence the mean and rms Nusselt number distributions at low *H/D*. When the vortices impinge upon the

surface at an early stage in their development, this promotes separation in the wall jet flow and the subsequent break-up of these strong vortices leads to large velocity fluctuations normal to the impingement surface. Vortices that impinge at later stages in their development are weaker and therefore as they break-up in the wall jet, the magnitude of the velocity fluctuations normal to the surface is reduced. This does not enhance the heat transfer in the wall jet, to the same degree as stronger vortices do. In general, the breakdown of strong vortices (in the early stages of the vortex development), has a favourable effect on the heat transfer in the near wall jet.

4. Conclusions

Results have been presented of fluid flow and heat transfer relating to an axially symmetric impinging air jet. It has been shown that at low nozzle to impingement surface spacings the mean heat transfer distribution exhibits secondary peaks that occur at a radial location. These peaks have been reported by several investigators and have been attributed, in general, to an abrupt increase in turbulence in the wall jet boundary layer. Results from the current investigation support this assertion. However the fluid mechanical processes that control the development of the wall jet boundary layer have not been well defined. Vortices that roll-up naturally in the shear layer of the free jet, close to the nozzle exit, have been shown to merge forming larger yet weaker vortices, before being broken down into smaller scale random turbulence. Stages within the merging processes have been identified to occur at various distances from the jet nozzle. Vortices eventually break down and the turbulence level within the wall jet increases significantly, which in turn increases the heat transfer, leading to a secondary peak in the heat transfer distribution.

5. Acknowledgements

This work was supported in part by Enterprise Ireland under grant SC/2001/0071 and also by Science Foundation Ireland grant 04/BR/EO108

6. References

1. Hollworth, B. R. and Durbin, M., 1992, “Impingement cooling of electronics,” *ASME Journal of Heat Transfer,* **114**, pp. 607 – 613.

2. Roy, S., Nasr, K., Patel, P. and AbdulNour, B., 2002, “An experimental and numerical study of heat transfer off an inclined surface subject to an impinging airflow,” *InternationalJournal of Heat and Mass Transfer,* **45**, pp. 1615 – 1629.

3. Babic, D. M., Murray, D. B. and Torrance, A. A., 2005, “Mist jet cooling of grinding processes,” *Accepted for publication in the International Journal of Machine Tools and Manufacture*.

4. Jambunathan, K., Lai, E., Moss, M. A. and Button, B. L., 1992, “A review of heat transfer data for a single circular jet impingement,” *International Journal of Heat Fluid Flow,* **13**, pp. 106 – 115.

5. Martin, H., 1977, “Heat and mass transfer between impinging gas jets and solid surfaces,” *Advances Heat Transfer,* **13**, pp. 1 – 60.

6. Polat, S., Huang, B., Mujumdar, A. S. and Douglas, W. J. M., 1989, “Numerical flow and heat transfer under impinging jets: a review,” *Annual Review of Numerical Fluid Mechanics Heat Transfer,* **2**, pp. 157 – 197.

7. Donaldson, C. D. and Snedeker, R. S., 1971, "A study of free jet impingement, part i mean properties of free impinging jets," *Journal of Fluid Mechanics,* **45**, pp. 281 – 319.

8. Beltaos, S. 1976, "Oblique impingement of circular turbulent jets," *Journal of Hydraulic Research,* **14**, pp. 17 – 36.

9. Gardon, R. J. and Akfirat, J. C., 1965, "The role of turbulence in determining the heat transfer characteristics of impinging jets," *International Journal of Heat and Mass Transfer,* **8**, pp. 1261 – 1272.

10. Baughn, J. W. and Shimizu, S. S., 1989, "Heat transfer measurements from a surface with uniform heat flux and an impinging jet," *ASME Journal of Heat Transfer,* **111**, pp. 1096 – 1098.

11. Huang, L. and El-Genk, M. S., 1994, "Heat transfer of an impinging jet on a flat surface," *International Journal of Heat and Mass Transfer,* **37**, pp. 1915 – 1923.

12. Goldstein, R. J., Behbahani, A. I. and Heppelmann, K., 1986, "Streamwise distribution of the recovery factor and the local heat transfer coefficient to an impinging circular air jet," *International Journal of Heat and Mass Transfer,***29**, pp. 1227 – 1235.

13. O'Donovan, T. S., Murray, D. B. and Torrance, A. A., 2005, "Impinging jet heat transfer in the transitional wall jet region," *Proceedings of ASME Summer Heat Transfer Conference*, San Francisco, Paper No. HT2005-72451

14. Hoogendoorn, C. J., 1977, "The effect of turbulence on heat transfer at a stagnation point," *International Journal of Heat and Mass Transfer,* **20**, pp. 1333 – 1338.

15. Goldstein, R. J. and Timmers, J. F., 1982, "Visualisation of heat transfer from arrays of impinging jets," *International Journal of Heat and Mass Transfer,* **25**, pp. 1857 – 1868.

16. Donaldson, C. D., Snedeker, R. S. and Margolis, D. P., 1971, "A study of free jet impingement. part ii. free jet turbulent structure and impingement heat transfer," *Journal of Fluid Mechanics,* **45**, pp. 477 – 512.

17. Mohanty, A. K. and Tawfek, A. A., 1993, "Heat transfer due to a round jet impinging normal to a flat surface," *International Journal of Heat and Mass Transfer,* **36**, pp. 1639 – 1647.

18. Fleischer, A. S., Kramer, K. and Goldstein, R. J., 2001, "Dynamics of the vortex structure of a jet impinging on a convex surface," *Experimental Thermal and Fluid Science,* **24**, pp. 169 – 175.

19. Hui, H., Kobayashi, T., Wu, S. and Shen, G., 1999, "Changes to the vortical and turbulent structure of jet flows due to mechanical tabs," *Proceedings of the Institution of Mechanical Engineers,* **213**, pp. 321 – 329.

20. Hussain, A. K. M. F., 1986, "Coherence structure and turbulence," *Journal of Fluid Mechanics,* **173**, pp. 303 – 356.

21. Liu, T. and Sullivan, J. P., 1996, "Heat transfer and flow structures in an excited circular impinging jet," *International Journal of Heat and Mass Transfer,* **39**, pp. 3695 - 3706.

22. Gao, N., Sun, H., and Ewing, D., 2003, "Heat transfer to impinging round jets with triangular tabs," *International Journal of Heat and Mass Transfer,* **46**, pp. 2557 - 2569.

23. Hwang, S. D., Lee, C. H. and Cho, H. H., 2001, "Heat transfer and flow structures in axisymmetric impinging jet controlled by vortex pairing," *International Journal of Heat and Fluid Flow,* **22**, pp. 293 - 300.

24. Hwang, S. D., and Cho, H. H., 2003, "Effects of acoustic excitation positions on heat transfer and flow in axisymmetric impinging jet: main jet excitation and shear layer excitation," *International Journal of Heat and Fluid Flow,* 24, pp. 199 - 209.

25. O'Donovan, T. S., 2005, "Fluid flow and heat transfer of an impinging air jet," *Ph.D. thesis, Department of Mechanical Engineering, University of Dublin, Trinity College*

26. Fitzpatrick, J. and Simon, L., 2005, "Estimation of cross-power spectra using sample-and-hold reconstruction of laser doppler anemometry data," *Accepted for Publication in Experiments in Fluids*.

27. Schadow, K. C., and Gutmark, E., 1992, "Combustion instability related to vortex shedding in dump combustors and their passive control," *Progress in Energy and Combustion Science,* **18**, pp. 117 – 132.

28. Han, B., and Goldstein, R. J., 2003, "Instantaneous energy separation in a free jet. part i. flow measurement and visualization," *International Journal of Heat and Mass Transfer,* **46**, pp. 3975 – 3981.

29. Broze, G., and Hussain, F., 1994, "Nonlinear dynamics of forced transitional jets: periodic and chaotic attractors," *Journal of Fluid Mechanics,* **263**, pp. 93 – 132.